Influence of interfacial texture on solid-state amorphization and associated asymmetric growth in immiscible Cu-Ta multilayers

H. R. Gong and B. X. Liu*

Advanced Materials Laboratory, Department of Materials Science and Engineering, Tsinghua University, Beijing 100084, China and State Key Laboratory of Solid-State Microstructures, Nanjing University, Nanjing 210008, China

(Received 21 November 2003; revised manuscript received 9 March 2004; published 12 October 2004)

For the immiscible Cu-Ta system, a Finnis-Sinclair potential is constructed and proven to be realistic in reproducing some static properties of the system. Applying the potential, molecular dynamics simulations reveal that among the nine Cu/Ta interfaces stacked by possible combinations of the (100), (110), and (111) atomic planes, the Ta (110) plane could remain stable up to a temperature of 600 °C, while the Cu (111) plane could remain unchanged only if combined with the Ta (100) and (110) planes. Simulations also show that for the other Cu/Ta interfaces, the interface energy serves as the driving force for interdiffusion of the Cu and Ta atoms across the interface, resulting in solid-state amorphization. Interestingly, it is calculated that the amorphization energy of Cu is smaller than that of Ta, thus resulting in an asymmetric growth behavior of the amorphous interlayer, i.e., amorphization of the Cu lattice is easier and faster than that of the Ta lattice. In general, the agreement between the simulation results and experimental observations is fairly good.

DOI: 10.1103/PhysRevB.70.134202 PACS number(s): 61.43.Dq, 82.20.Wt

I. INTRODUCTION

Since the first discovery of solid-state amorphization (SSA) in the Au-La system in 1983,[1] significant progress has been achieved in both experimental studies and theoretical modeling.[2] For the binary metal systems characterized by negative heats of formation (ΔH_f),[3] molecular dynamics (MD) simulations have been employed to reveal the atomistic mechanism of the interfacial reaction and resultant SSA between the miscible metals.[4] For the equilibrium immiscible systems characterized by positive ΔH_f, a number of experimental studies have demonstrated the possibility of the interfacial reaction as well as SSA, and thermodynamic calculations have confirmed the decisive role of the interface energy in driving the interfacial reaction as well as SSA.[5,6] Nonetheless, a clear understanding of the interfacial reaction and SSA between the immiscible metals at an atomistic scale is still lacking. Consequently, the scientific issue of interface stability is of general interest and requires further studies. The present work is dedicated to develop an atomistic model for the thermal stability of the interfaces in the equilibrium immiscible systems by choosing the Cu-Ta system as a representative one based on following considerations. The Cu-Ta system is characterized with a positive ΔH_f of +3 kJ/mol and has drawn special attention due to its hi-tech application, i.e., a thin Ta layer has been used as a diffusion barrier to prevent Cu from diffusing into Si and GaAs underneath in ultralarge scale integration devices and field-effect transistors, respectively.[7,8] The questions related to the Cu-Ta system are therefore first, whether or not interfacial reaction at the Cu/Ta interface can take place and second, what is the controlling factor that would enhance or suppress the reaction, which, if it takes place, would certainly degrade the device performance. In addition, there has been a controversy concerning the behaviors of Cu/Ta interfaces observed in experiments by different researchers, e.g., some researchers showed that SSA took place at the Cu/Ta interfaces upon annealing within a temperature range of 400–600 °C,[9–11] whereas some researchers claimed that the Cu/Ta interfaces could be thermally stable up to a temperature of 600 °C.[7,12,13] Such a controversy also requires a relevant atomistic model for clarifying the interface stability of the Cu-Ta system. The present study is dedicated to investigate the above issues in detail through MD simulation on the basis of a very recent work by the authors' group.[14]

To perform MD simulation in a binary metal system, a realistic potential of the system is necessary and should first be constructed. Previously, there have been two embedded-atom Cu-Ta potentials reported in the literature,[15,16] however, the potentials were derived for studying some other issues and did not show the capability of revealing the solid-state reaction at the Cu/Ta interfaces. Very recently, another *n*-body Cu-Ta potential under the Finnis-Sinclair (FS) formalism was constructed in a Letter by the present authors.[14] In this paper, we further present the detailed construction process as well as the validation of this Cu-Ta potential. Appling the potential, MD simulations are then performed with nine sandwich models and a bilayer model to reveal the effect of interfacial texture on solid-state reaction and the detailed kinetics of amorphization upon isothermal annealing at medium temperatures ranging from 200 to 600 °C.

II. CONSTUCTION OF AN *N*-BODY POTENTIAL

In 1984, Finnis and Sinclair (FS) proposed a simple empirical *n*-body potential based on the second-moment approximation and successfully constructed the potentials for some bcc transition metals.[17] Later, the so-called FS formalism has been employed to study the physical properties of some bcc and fcc metals as well as alloys in a satisfactory way.[4,18–23] In construction of the Cu-Ta potential under the FS formalism,[17] the total energy of a system is given by

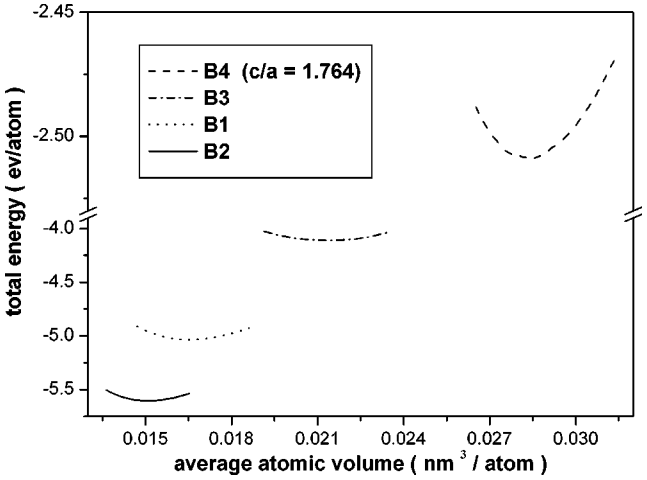

FIG. 1. The *ab initio* calculated total energy versus average atomic volume for the CuTa compound in different structures.

$$U_{\text{tot}} = \frac{1}{2}\sum_{ij} V(r_{ij}) - \sum_{i}\left[\sum_{j\neq i} A^2\phi(r_{ij})\right]^{1/2}, \tag{1}$$

where the first term is a normal pairwise energy consisting of a repulsive part, the second term is the *n*-body term taking a sum form over all atoms for a "cohesive function," and A is a positive constant to be fitted. In Eq. (1), $V(r_{ij})$ is the pair potential between atom i and j taking the quartic polynomial and $\phi(r_{ij})$ is the cohesive potential between atom i and j taking the parabolic form, as follows:

$$V(r) = \begin{cases} (r-c)^2(c_0 + c_1 r + c_2 r^2), & r \leqslant c, \\ 0, & r > c, \end{cases} \tag{2}$$

$$\phi(r) = \begin{cases} (r-d)^2, & r \leqslant d, \\ 0, & r > d, \end{cases} \tag{3}$$

where c and d are two disposable parameters assumed to be between the second- and third-neighbor distances, and c_0, c_1, and c_2 are three parameters to be fitted.

The Cu-Cu and Ta-Ta potentials are fitted to some experimental data of Cu and Ta, such as the cohesive energies, lattice constants, and shear elastic constants. It should be pointed out that in the equilibrium immiscible Cu-Ta system, there is no any equilibrium compound and therefore no indispensable data available for fitting the Cu-Ta cross potential. In this respect, the first-principles calculation based on quantum mechanics is a reliable way for acquiring some physical properties of the equilibrium as well as nonequilibrium alloy phases.[24,25] We, therefore, performed the first-principles calculations, based on the well-established Vienna *ab initio* simulation package (VASP),[26] to obtain the cohesive energies and lattice constants of nonequilibrium CuTa and Cu_3Ta compounds for fitting the Cu-Ta cross potential. Concerning the details of *ab initio* calculation, the readers are referred to the authors' recent paper.[16] Accordingly, the calculated total energy versus the average atomic volume for the nonequilibrium CuTa compound in several possible structures, respectively, is shown in Fig. 1. It can be seen that the CuTa compound in a $B2$ structure has the lowest energy among the four calculated structures. Meanwhile, similar calculations indicate that the Cu_3Ta compound in a $L1_2$ structure shows a lower energy, comparing with other possible structures (calculated curves not shown). As a result, the cohesive energies of the nonequilibrium $B2$ CuTa and $L1_2$ Cu_3Ta compounds are 5.604 and 4.325 eV, respectively, and their lattice constants are 3.11 and 3.82 Å, respectively. These computed data are then applied in fitting the Cu-Ta cross potential. After the fitting procedure and optimization of the potential parameters, Table I lists the fitted parameters for the Cu-Cu, Ta-Ta, and Cu-Ta potentials.[14] Table II shows the comparison between some physical properties reproduced by the constructed potentials and the experimental/*ab initio* values used initially for fitting the potentials. It can be seen that the constructed Cu-Ta potentials work fairly well in terms of reproducing some physical properties of the pure Cu and Ta, as well as the nonequilibrium CuTa and Cu_3Ta compounds in the system.

TABLE I. The fitted parameters for Cu-Cu, Ta-Ta, and Cu-Ta potentials (Ref. 14).

	Cu-Cu	Ta-Ta	Cu-Ta
A (eV)	1.43342334	2.54410095	0.74825821
d (Å)	3.62	4.15	5.06
c (Å)	3.75	3.6	4.49
c_0	3.47785160	1.52167356	0.58981438
c_1	−2.37546941	0.28773159	−0.19540066
c_2	0.42773951	−0.14981772	0.0

We now turn to testify the relevance of the constructed Cu-Ta potential. We first calculate some physical properties of the $CuTa_3$ compound in a $L1_2$ structure from *ab initio* calculation and from the Cu-Ta potential, respectively. Table II lists the calculated results for the $L1_2$ $CuTa_3$ compound. One sees clearly from the table that the lattice constants derived from *ab initio* calculation and the Cu-Ta potential match well with each other, as the difference between them is only about 3.2%. Moreover, the cohesive energy of the $L1_2$ $CuTa_3$ compound deduced from the potential is 6.97 eV, which is in good agreement with the value of 6.80 eV predicted by *ab initio* calculation, as their difference is only about 2.5%. It should be emphasized that the related properties of the $L1_2$ $CuTa_3$ compound obtained by *ab initio* calculation have not been used in fitting the Cu-Ta cross potential. Consequently, such a good agreement could lend firm support to the relevance of the newly constructed Cu-Ta potential. In addition, MD simulation is conducted to calculate the heats of formation (ΔH_f) of the metastable fcc/bcc Cu-Ta solid solutions over the entire composition range upon annealing at 0 K. Regarding the detailed settings of the fcc/bcc solid solution models, the readers are referred to our recent published paper.[30] The calculation results show that the ΔH_f of the metastable fcc/bcc Cu-Ta solid solutions over the entire composition range are all positive, e.g., the ΔH_f of the fcc and bcc CuTa solid solutions are 8.46 and 2.64 kJ/mol, respectively. It should be pointed out that such a positive ΔH_f derived from the present Cu-Ta potential is compatible

TABLE II. Comparison between calculated values and experimental data/*ab initio* results of the cohesive energy E_c (eV), lattice constant a (Å), and elastic constants (Mbar) in the Cu-Ta system. The values of the $L1_2$ $CuTa_3$ are used to testify the relevance of the Cu-Ta potential.

Phase	Structure	Method	E_c (eV)	a (Å)	C_{11} (Mbar)	C_{12} (Mbar)	C_{44} (Mbar)
Cu	FCC	Exp.	3.54[a]	3.615[a]	1.70[a]	1.225[a]	0.758[a]
		This work	3.54	3.615	1.70	1.222	0.759
Ta	BCC	Exp.	8.089[b]	3.3026[b]	2.66[c]	1.58[c]	0.87[c]
		This work	8.006	3.3026	2.69	1.60	0.87
CuTa	B2	*Ab initio*	5.604	3.11			
		Fitted	5.600	3.13			
Cu_3Ta	$L1_2$	*Ab initio*	4.325	3.82			
		Fitted	4.308	3.74			
$CuTa_3$	$L1_2$	*Ab initio*	6.80	4.05			
		Potential	6.97	4.18			
		Difference	2.5%	3.2%			

[a]Reference 27.
[b]Reference 28.
[c]Reference 29.

with that deduced from the thermodynamics of solids,[3] and may also validate the newly constructed Cu-Ta potential.

III. SIMULATION MODELS

A. Bilayer model

To study the detailed process of SSA in the Cu-Ta interface, a bilayer model of [8Cu(110)/8Ta(100)] is constructed by sequentially stacking eight fcc Cu (110) planes (Nos. 1–8) and eight bcc Ta (100) planes (Nos. 9–16) along the z direction. The [110] direction of the Cu lattice and the [100] direction of the Ta lattice are arranged to be parallel to the x direction, respectively, while both [010] direction of the Cu and Ta lattices is parallel to the y axis. In other words, an interface is thus created in the x-y plane by approaching a Ta lattice to a Cu lattice.

The sizes of the lattices, in the x-y plane, are chosen to have a mismatch at the Cu-Ta interface as close as possible to the real ratio of their crystal lattices. It is known that the lattice constants of the Cu and Ta crystals are 3.615 and 3.3026 Å, respectively, and the ratios of atomic distances in Cu(110)/Ta(100) are approximately 0.774 and 1.095 in the x and y directions, respectively. Considering a manageable scale of the computation in the present study, the numbers of Cu and Ta unit cells in their respective planes are selected to be $10\times12\times1=120$ for the Ta (100) plane and $13\times11\times1=143$ for the Cu (110) plane, corresponding to the ratios of $10/13=0.769$ and $12/11=1.091$ in the x and y direction, respectively, which are quite close to the real situation. In the bilayer model, there are altogether 2104 atoms, i.e., $143\times8=1144$ Cu atoms and $120\times8=960$ Ta atoms. For the boundary conditions, in the x and y directions, both periodic conditions are imposed with a larger dimension of the Cu and Ta lattices, respectively, i.e., the Cu (110) and (010) in the x and y direction, respectively. While in the z direction, a free boundary condition is adopted to avoid the otherwise influence on the process of SSA from having another interface in the model. It is estimated that a misfit caused by a difference between the dimensions of the Cu and Ta lattices and the periodic conditions along the x and y directions will result in at most a 1% decreasing of Ta density in the models. In this regard, as pointed out by Mura *et al.*[31] such a minor reduction in density has no considerable influence on the simulation results.

To have the bilayer model with a starting configuration similar to a real situation such as that observed in experiments, i.e., an amorphous interlayer was formed during the deposition of the thin films,[8,10,32] an initially disordered interlayer was introduced by randomly exchanging an equal number of Cu and Ta atoms in the interlayer. To characterize quantitatively the amount of disordering created by exchanging atoms, the concept of long-range order (LRO) parameter originally proposed to describe the ordering in crystalline alloys[33] was employed in the present study. The LRO parameter is defined as $\eta=(p-\gamma)/(1-\gamma)$, where p and γ are the probability of the presence of an A type atom (A=Cu or Ta) on its own lattice site and the molar ratio of A atoms, respectively, both in the initial interlayer. Values $\eta=0$ and 1 correspond, respectively, to a completely chemical disordering or to an entirely ordered crystalline state. Such a disordered interlayer is preset in two atomic planes consisting of one Cu and one Ta planes next to each other.

B. Sandwich models

To study the effect of interfacial texture on solid-state reaction, Ta-Cu-Ta sandwich models with different crystalline orientations of the Cu and Ta lattices are constructed for simulation. Nine Ta-Cu-Ta sandwich models with possible combinations of the Cu (100), (110), and (111) planes with the Ta (100), (110), and (111) planes are constructed by

stacking a specific number of Cu and Ta atomic planes along the *z* axis and are abbreviated by the following symbols: [4Ta (100)/6Cu (100)/4Ta (100)], [4Ta (110)/6Cu (100)/4Ta (110)], [6Ta (111)/8Cu (100)/6Ta (111)], [6Ta (100)/8Cu (110)/4Ta (100)], [4Ta (110)/8Cu (110)/4Ta (110)], [6Ta (111)/8Cu (110)/6Ta (111)], [6Ta (100)/9Cu (111)/6Ta (100)], [4Ta (110)/9Cu (111)/4Ta (110)], and [6Ta (111)/6Cu (111)/6Ta (111)]. To each Cu-Ta sandwich model, two interfaces between Cu and Ta lattices are introduced as follows. When a Cu lattice and a Ta lattice approach each other along the *z* direction, an interface is created in the *x*-*y* plane and another interface is introduced by approaching another Cu lattice to the same Ta lattice from the other direction.

Similar to the setting of the [8Cu (110)/8Ta (100)] bilayer model, the sizes of the lattices, in the *x*-*y* plane, are chosen to have a mismatch at the Cu-Ta interface as close as possible to the real ratio of their crystal lattices. The size of the corresponding computational block in the *z* direction is obtained by varying the distances between the Cu and Ta lattices to an optimized value corresponding to a minimum enthalpy for each model. For the boundary conditions, in the *z* direction, a periodic condition is imposed, and two Ta lattices in a sandwich model are therefore adhered together to form a united lattice. While in the *x* and *y* direction, the larger one of the Cu and Ta lattice dimensions is adopted to set the periodic boundary conditions. Consequently, the computational block of a sandwich model is a representative unit of compositionally modulated multilayers and simulation of such a sandwich model is in fact to simulate the Cu-Ta multilayers, which are usually employed in experiments for studying solid-state reaction and amorphization.

To find out the role of interfacial disordered layer in SSA, we also artificially introduce a disordered layer by exchanging an equal number of Cu and Ta atoms in the interfaces to surpass the necessary stage of nucleation at the interfaces for growing an amorphous phase. In addition, the LRO parameter η is varied from 0 to 1 to find out the influence of the preset disordered layer on the SSA of the interfaces.

IV. COMPUTATION AND CHARACTERIZATION

Based on the constructed Cu-Ta potential, MD simulation with the bilayer and sandwich models is carried out with a Parrinello-Rahman constant pressure scheme and the equations of motion are solved using a fourth-order predictor-corrector algorithm of Gear with a time step of $t=5\times10^{-15}$ s.[34] The simulation starts by equilibrating the model at room temperature (27 °C) for 5000 MD time steps to reach an equilibrium configuration as an initial state. From the initial state, the temperature of the models is raised, by boosting the velocities of the atoms to the desired simulation temperature ranging from 200 to 600 °C, at which the models are then isothermally annealed. As the velocities of the atoms will change during annealing, a time-to-time rescaling of the velocities to the assigned temperature is executed at every 100 MD time steps, if an average deviation from the assigned temperature is over 1 °C.

The process of the interfacial reaction and SSA in the Cu-Ta bilayer and sandwich models is monitored by the projections of the atomic positions, the planar structure factor $S(\mathbf{k})$, the pair-correlation function $g(r)$, as well as the density profiles of each species along the *z* direction $\rho_\alpha(z)$. The planar structure factor $S(\mathbf{k})$ is a Fourier transformation of the density to characterize the long-range order in the direction of any vector $\mathbf{k}$, which is a vector of the reciprocal space lattice. Accordingly, the planar structure factor $S=1$ refers to an entirely ordered crystal, while $S=0$ is for a completely disordered state.[35] In the present study, we choose $S(\mathbf{k},\mathbf{z})$, as a specific representative of $S(\mathbf{k})$, to reflect the structural phase transition in each crystallographic plane parallel to the *x*-*y* plane. As one of the main criteria to determine an amorphous structure, $g(r)$ is commonly used to identify the structure of a block material by sampling the atoms involved in the block.[36] $\rho_\alpha(z)$ is calculated to define the position of a single atomic layer, indicating the local structural and compositional properties of the models.[37]

V. RESULTS AND DISCUSSION

A. Influence of interfacial texture on solid-state reaction

Applying the constructed Cu-Ta potential, MD simulation is first conducted to study the thermal stability of the Cu/Ta interfaces through annealing all nine sandwich models at 600 °C. For all the models, a disordered interlayer is preset at the interfaces and the LRO parameter η is set to be the same value of 0.1. Accordingly, the simulation results for the nine sandwich models are summarized and listed in Table III.[14] It can be seen that the interfacial texture has strong influence on the thermal stability and solid-state reaction of the Cu/Ta interfaces, i.e., the Cu/Ta interface with different textures may have quite different behaviors in interfacial reaction upon the same annealing conditions. Briefly speaking, the Cu/Ta interfaces can be classified into three categories in terms of their thermal stability, i.e., the stable Cu (111)/Ta (100) and Cu (111)/Ta (110) interfaces, the partially stable Cu (100)/Ta (110) and Cu (110)/Ta (110) interfaces, and the remaining unstable interfaces. Moreover, the Cu and Ta atomic planes have different characteristics concerning thermal stability. That is to say, the most stable atomic plane of the Ta lattice is the (110) plane which could all remain stable with combinations of Cu (100), (110), and (111) atomic planes, while the most stable plane of the Cu lattice is the (111) plane, which could remain unchanged only if combined with the Ta (100) and (110) planes.

It is of interest to compare the above simulation results with some experimental observations. As presented in the Introduction, a controversy appeared in the experimental results reported so far in the literature, i.e., some reports showed that solid-state reaction took place at the Cu/Ta interfaces upon annealing at 400–600 °C,[9–11] whereas some other reports claimed that the Cu/Ta interfaces were stable up to 600 °C.[7,12,13] Apparently, such an experimental discrepancy could be clarified by the above simulation results, which demonstrate that it is the different interfacial textures of the Cu/Ta interfaces that result in the different behaviors

TABLE III. Interfacial texture on thermal stability of the Cu/Ta interfaces upon annealing at 600 °C. The relative interface energies, ΔE^I, calculated at 0 K are also listed and the interface energy of the Cu(111)/Ta(110) interface is defined as the ground reference state (Ref. 14).

Interface	Simulation result	Stability of Cu plane	Stability of Ta plane	ΔE^I (J/m^2)
Cu(111)/Ta(110)	Stable	Yes	Yes	0
Cu(111)/Ta(100)	Stable	Yes	Yes	0.3456
Cu(100)/Ta(110)	Partially stable	No	Yes	0.1429
Cu(110)/Ta(110)	Partially stable	No	Yes	0.2195
Cu(100)/Ta(100)	Unstable	No	No	0.4575
Cu(110)/Ta(100)	Unstable	No	No	0.5140
Cu(111)/Ta(111)	Unstable	No	No	0.4816
Cu(100)/Ta(111)	Unstable	No	No	0.5440
Cu(110)/Ta(111)	Unstable	No	No	1.8256

of the interfacial reactions.[7,9–13] In addition, there are also some direct experimental evidence regarding the effect of interfacial texture on Cu/Ta interfacial reactions.[38–40] For instance, Kuhn *et al.* prepared a Cu (111)/Ta (110)-like interface and found that Cu and Ta did not react to form any alloy.[38] Hoogeveen *et al.* observed that the sputter-deposited Cu/Ta multilayers favored the Cu (111)/Ta (110) and Cu(111)/Ta (100) textures.[39] Chin *et al.* also observed that the Ta/Cu/Ta multilayers exhibited a highly Cu (111)-preferred crystalline structure.[40] It should be noted that the above experimental observations are in good agreement with the present MD simulation results, signifying that the Cu (111)/Ta (100) and Cu (111)/Ta (110) interfaces are preferably formed and can remain stable upon annealing. Such a good agreement provides further support to the validation of the constructed Cu-Ta potential, and also suggests that only Cu (111)/Ta (100) and Cu (111)/Ta (110) interfaces could be considered as diffusion barrier couples to be applied in the electronic devices up to a temperature of about 600 °C.

It should be emphasized that as described above, to simulate the experimentally observed amorphous interlayer appearing in the interfaces,[8,10,32] a disordered interlayer is preset in the interfaces for all the sandwich models in the present simulation. Under such a uniform condition, simulation results displayed in Table III suggest that the interfacial texture has strong influence on the thermal stability and solid-state reaction of the Cu/Ta interfaces. That is to say, the Cu (111)/Ta (100) and Cu (111)/Ta (110) interfaces could remain stable upon annealing at 600 °C. These results suggest that these two interfaces can serve as both nucleation and growth barriers for solid-state reaction, which is in good agreement with some experimental observations.[7,12,13,38] While the other interfaces, such as Cu (100)/Ta (100), etc., are prone to solid-state reaction upon annealing, which is also in agreement with some other experimental results.[9–11]

To find out the reason for the important effect of the interfacial texture on solid-state reaction, the interface energy E^I of the nine Ta-Cu-Ta sandwich models is calculated by the following formula:

$$E^I = \frac{E^m - N_{\mathrm{Cu}}E^{\mathrm{coh}}_{\mathrm{Cu}} - N_{\mathrm{Ta}}E^{\mathrm{coh}}_{\mathrm{Ta}}}{\text{interfacial area}}, \tag{4}$$

where E^m is the energy of a sandwich model with no preset disordered interlayer after relaxation at 0 K, N_{Cu} and N_{Ta} are the numbers of Cu and Ta atoms in the sandwich model, respectively, and $E^{\mathrm{coh}}_{\mathrm{Cu}}$ and $E^{\mathrm{coh}}_{\mathrm{Ta}}$ are the cohesive energies of Cu and Ta, respectively. As the calculated interface energy of the sandwich model [4Ta (110)/9Cu (111)/4Ta (110)] constructed by stacking both the close-packed atomic planes of Cu and Ta has the lowest value, we define it as a ground reference state and set its energy zero. Accordingly, the relative interface energies of other simulation models are therefore derived and also listed in Table III. One sees from the table that for the partially stable and unstable Cu/Ta interfaces the interface energy could serve as the driving force for the interfacial reaction. One also sees that generally speaking, the thermal stability of the Cu/Ta interfaces is strongly correlated with the interface energy, i.e., with the increase of the interface energy the interface becomes from stable to partially stable, and then from partially stable to unstable. The only exception of the above statement is the stable Cu (111)/Ta Ta (100) interface, which has higher energy than the partially stable Cu(100)/Ta(110) interface. This, to the authors' view, may imply that the critical energy for triggering the interfacial reaction has something to do with the interfacial texture, i.e., different atomic planes may need different critical energy to drive the interfacial reaction. Interestingly, there is indeed some experimental evidence in the literature regarding interfacial reaction of some immiscible systems. For instance, Zhang *et al.* performed thermodynamic calculations and found that the interface energy in the Y-Mo and Ag-Mo multilayered films elevated the energetic states of the films up to higher energy level than that of the amorphous state, signifying the feasibility of forming amorphous alloys in the films simply by thermal annealing.[41,42] It should be emphasized that these experimental observations match well with the present simulation results, i.e., a sufficiently high interface energy could serve as the driving force

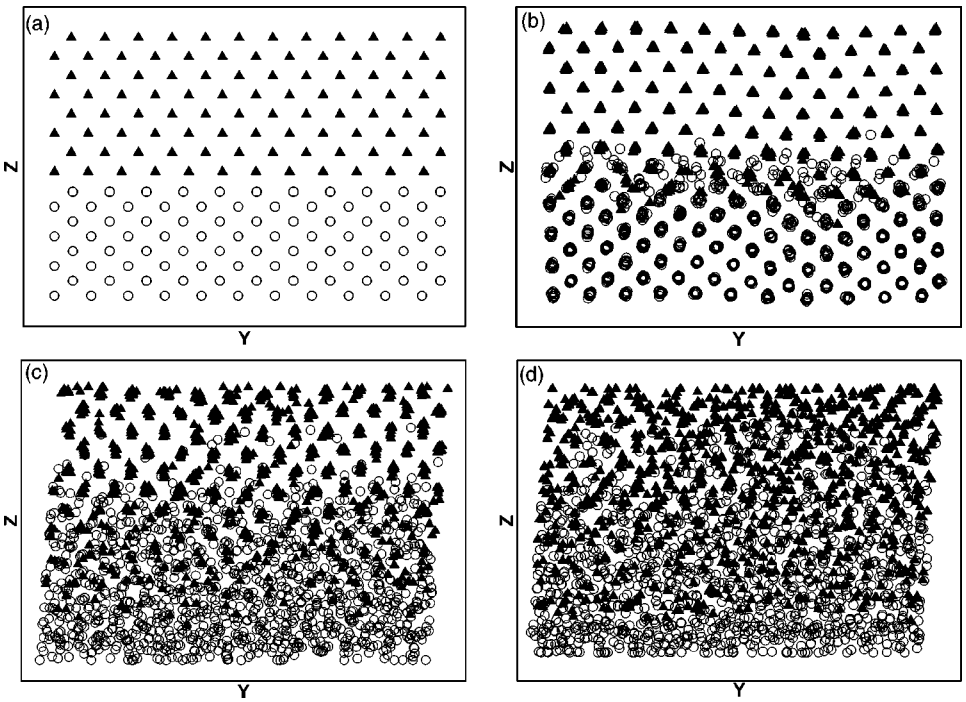

FIG. 2. The projections of atomic positions on the *y*-*z* plane of the bilayer model of [8Cu(110)/8Ta(100)] after annealing (a) at 27 °C for 0 MD time step, (b) at 27 °C for 5000 MD time steps, (c) at 600 °C for 5000 MD time steps, and (d) at 600 °C for 20 000 MD time steps. Open circles: Cu. Filled triangles: Ta.

for the interfacial reaction in the equilibrium immiscible systems.

B. Atomic diffusion and interfacial amorphization

To present some detailed process of interfacial amorphization, we first show the simulation results obtained in the bilayer model constructed in a configuration of [8Cu(110)/8Ta(100)] after isothermal annealing at 600 °C. Accordingly, the projections of atomic positions of the bilayer model on the *y*-*z* plane before annealing is shown in Fig. 2(a). One observes vividly that eight Cu (110) planes and eight Ta (100) planes are sharply separated by the Cu/Ta interface. The initial state of the bilayer model after annealing at 27 °C for 5000 MD time steps is displayed in Fig. 2(b) by the projections of atomic positions on the *y*-*z* plane, from which the crystalline structures of the Cu and Ta lattices are clearly discerned, although the thermal vibration causes some minor movements of the atoms. As mentioned before, a disordered layer is artificially introduced into the Cu/Ta interface and the LRO parameter η is set, in the present bilayer model, to be 0.1, which results in an exchange of 58 Cu (Ta) atoms in the interface. From the initial state, the model is then annealed at 600 °C. Figures 2(c) and 2(d) are the projections of the atomic positions on the *y*-*z* plane after annealing the model for 5000 and 20 000 MD time steps, respectively, and from the figures, the disordering process can clearly be visualized. Figure 2(c) indicates that the Cu (Ta) atoms have diffused into the Ta (Cu) lattice through the Cu/Ta interface, and that the number of Ta atoms diffusing into the Cu lattice is more than that of the Cu into the Ta lattice, which results in a disordered state of the Cu lattice, while the Ta lattice remains its bcc structure. Figure 2(d) shows that upon further annealing, more Cu atoms have diffused into the Ta lattice and consequently, the Ta lattice collapses into a disordered state, resulting in a uniform amorphous structure of the bilayer model. To confirm the resultant amorphous state, four sets of partial and total pair-correlation functions $g(r)$ for the bilayer model after annealing at 600 °C for 20 000 MD time steps are calculated and shown in Fig. 3. It can be seen that the pair-correlation function curves apparently feature the shapes commonly known for an amorphous alloy.

From the above observations, it can be summarized that the interdiffusion of the Cu and Ta atoms across the Cu(110)/Ta(100) interface upon annealing gives rise to the collapsing of the Cu and Ta lattices as well as the complete

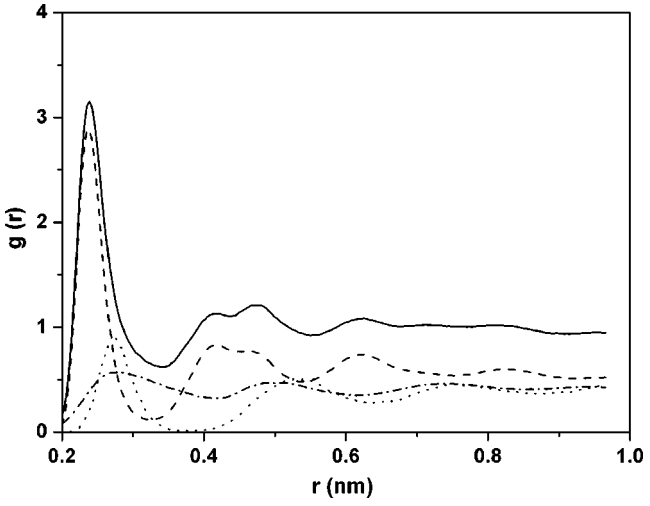

FIG. 3. Partial and total pair correlation functions of the bilayer model of [8Cu(110)/8Ta(100)] after annealing at 600 °C for 20 000 MD time steps. The solid line is for total $g(r)$, dashed line is for Cu-Cu partial $g(r)$, dotted line is for Ta-Ta partial $g(r)$, and dash-dotted line is for Cu-Ta partial $g(r)$.

amorphization of the Cu/Ta interface, and that diffusion of Ta atoms into Cu is faster than diffusion of Cu atoms into Ta. Interestingly, Lee *et al.*, by using high-resolution electron microscopy (HREM) and nanoprobe energy-dispersive spectroscopy (EDS), have directly observed the interdiffusion between Cu and Ta, which resulted in SSA near the Cu/Ta interface, and found that diffusion of Ta into Cu was faster than diffusion of Cu into Ta.[43] Apparently, these experimental observations are in excellent agreement with the above simulation results and provide firm support for the relevance of the newly constructed Cu-Ta potential as well as the present simulation regarding the SSA of the Cu/Ta interface.

We now discuss a little further concerning the interdiffusion of the Cu and Ta atoms across the Cu/Ta interface. It is well known that in the equilibrium immiscible Cu-Ta system, the Cu and Ta atoms are repulsive, and that the solid solubilities, for both Cu in Ta and Ta in Cu, are almost negligible.[3] The question is thus raised: why the Cu and Ta atoms could diffuse across the Cu/Ta interface? As shown in Table III, the answer is revealed at an atomistic scale in the present study, i.e., it is the high interface energy that serves as the driving force for the interdiffusion of Cu and Ta across some Cu/Ta interfaces. On the other hand, however, the interface energy stored in the stable Cu(111)/Ta(100) and Cu(111)/Ta(110) interfaces is not high enough to trigger the interdiffusion of Cu and Ta atoms and therefore interfacial amorphization could not happen upon annealing.

C. Asymmetric growth of amorphous interlayer

It is found that during the SSA of the Cu/Ta interfaces, there appears an asymmetric growth behavior of the amorphous interlayer, i.e., in the Cu(100)/Ta(110) and Cu(110)/Ta(110) interfaces, SSA only takes place in the Cu lattice, but not in the Ta lattice, and in the Cu(100)/Ta(100), Cu(100)/Ta(111), Cu(110)/Ta(100), Cu(110)/Ta(111), and Cu(111)/Ta(111) interfaces, the growing speed of the amorphous interlayer toward the Cu lattice is greater than that toward the Ta lattice.

As a typical example, we first show the simulation results of the sandwich model of [4Ta(110)/6Cu(100)/4Ta(110)] after annealing at 600 °C. In the sandwich model, there are altogether 2532 atoms, i.e., $9\times11\times6\times2=1188$ Cu atoms and $7\times12\times8\times2=1344$ Ta atoms, and 14 atomic planes stacking along the z axis, i.e., four Ta (110) planes (Nos. 1–4), six Cu (100) planes (Nos. 5–10), and also four Ta (110) planes (Nos. 11–14). As mentioned before, a disordered layer is artificially introduced into each of the two Cu/Ta interfaces and the LRO parameter η is set to be 0.1, which results in an exchange of 81 Cu (Ta) atoms in each interface. Accordingly, Fig. 4 displays two projections of the atomic positions on the y-z plane after annealing at 600 °C for 0 and 100 000 MD time steps, respectively. From the projections, one sees that after annealing at 600 °C, the Cu lattice is in a completely disordered state, while the Ta lattice remains a crystalline structure, showing an asymmetric growth behavior of the amorphous interlayer. To give further evidence, four sets of partial and total pair-correlation functions $g(r)$ for the Cu and Ta lattices after annealing at 600 °C for 100 000 MD time steps are calculated, respectively, and shown in Fig. 5. It can be seen that the $g(r)$ curves of the Cu lattice exhibit the typical shapes for an amorphous state, while the curves of the Ta lattice display the typical shapes for a crystalline state, corresponding to the asymmetric growth behavior displayed in Fig. 4(b).

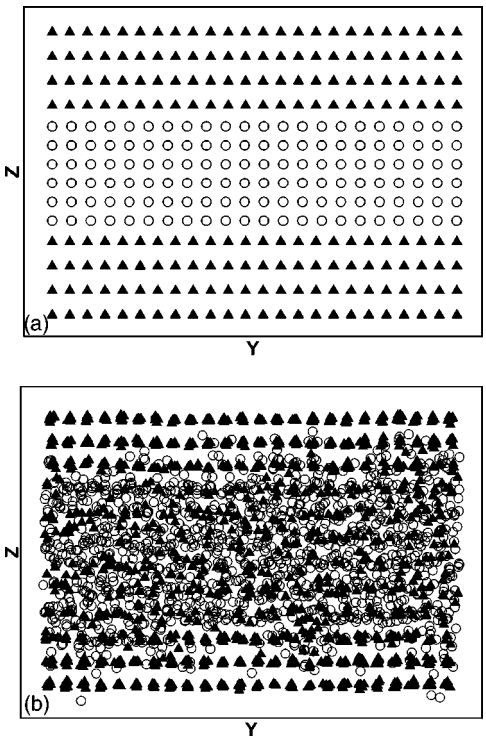

FIG. 4. The projections of atomic positions on the y-z plane for the sandwich model of [4Ta(110)/6Cu(100)/4Ta(110)] after annealing at 600 °C for (a) 0 MD time step and (b) 100 000 MD time steps. Open circles: Cu. Filled triangles: Ta.

We now discuss a little more about the simulation results for another typical sandwich model of [4Ta(100)/6Cu(100)/4Ta(100)] upon annealing at 350 °C. In this sandwich model, both the Cu and Ta lattices could become amorphous, while the growing speed of the amorphous interlayer toward the Cu lattice is greater than that toward the Ta one, signifying an asymmetric growth behavior of the amorphous interlayer. As a result, the planar structure factors of the 14 atomic planes in the sandwich model are calculated at various MD time steps and are shown in Fig. 6. One sees that after annealing at 350 °C for 10 000 MD time steps, the $S(\mathbf{k},\mathbf{z})$ values of the Cu lattice (Nos. 5–10) are reduced from about 1.0 of the initial state to almost 0, while the $S(\mathbf{k},\mathbf{z})$ values of the Ta lattice (Nos. 1–4 and 11–14) are still greater than 0.1, illustrating that the Cu lattice has become amorphous, while the Ta lattice is still in a crystalline state. One also sees that after annealing at 350 °C for 35 000 MD time steps, the $S(\mathbf{k},\mathbf{z})$ values of the Ta lattice are also reduced to almost 0, signifying that all the 14 atomic planes in the sandwich model have turned amorphous. To express the asymmetric growth quantitatively, the detailed growth kinetics of SSA are monitored and the calculation results show that the growing speed of the amorphous interlayer toward the Cu lattice is 43.38×10^{-5} m/s, which is

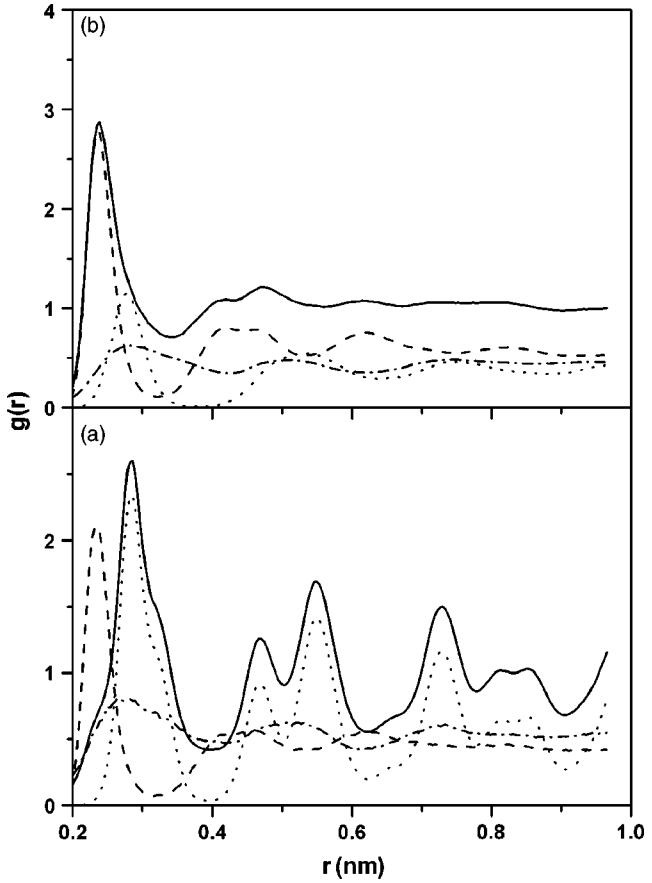

FIG. 5. Partial and total pair correlation functions for (a) The Ta lattice (Nos. 1–4) and (b) The Cu lattice (Nos. 5–10) of the sandwich model of [4Ta(110)/6Cu(100)/4Ta(110)] after annealing at 600 °C for 100 000 MD time steps. The solid line is for total $g(r)$, dashed line is for Cu-Cu partial $g(r)$, dotted line is for Ta-Ta partial $g(r)$, and dash-dotted line is for Cu-Ta partial $g(r)$.

about six times of 6.61×10^{-5} m/s calculated for that toward the Ta lattice. Moreover, as shown in Fig 6, the disordering process of the Cu lattice is completely prior to that of the Ta lattice, it is possible to calculate the amorphization energies of the Cu and Ta separately. For the sandwich model of [4Ta(100)/6Cu(100)/4Ta(100)] upon annealing at 350 °C, the amorphization energy of Cu is calculated to be 0.1123 eV/atom and the amorphization energy of Ta is figured out to be 0.3495 eV/atom. It should be noticed that the amorphization energy of Cu is about one third of that of Ta. Such a difference between the amorphization energies of Cu and Ta suggests that Cu is far easier to become amorphous than Ta, and could also bring about a reasonable explanation to the asymmetric growth of SSA observed in the above MD simulation.

Interestingly, based on the experimental studies, Kwon *et al.* reported that in the Cu-Ta interface, SSA proceeded primarily in the Cu lattice.[10] Obviously, Kwon's experimental observation is in excellent agreement with the asymmetric amorphization revealed by the present Cu-Ta potential. Moreover, the verdict revealed in the present MD simulation, i.e., the amorphization energy of Cu is greater than that of Ta, could also provide a physical explanation to the asymmetric amorphization behavior observed experimentally in the Cu-Ta system.[10]

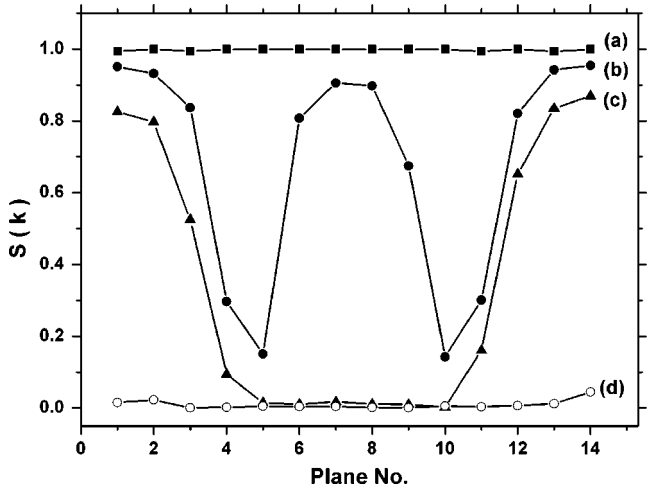

FIG. 6. The planar structure factors $S(\mathbf{k},\mathbf{z})$ for the sandwich model of [4Ta(100)/6Cu(100)/4Ta(100)] after annealing (a) at 27 °C for 0 MD time step, (b) at 27 °C for 5000 MD time steps, (c) at 300 °C for 10 000 MD time steps, and (d) at 350 °C for 35 000 MD time steps.

Finally, we discuss briefly the effect of annealing temperature and chemical disordering on the SSA of the Cu/Ta interface. Generally speaking, the amorphization of a specific Cu/Ta interface is speeded up with increasing the annealing temperature and the minimum annealing temperature (onset temperature) for the amorphization of Cu is less than that for the amorphization of Ta. To the Cu(110)/Ta(111) interface with the highest interface energy among the nine Cu/Ta interfaces, the interfacial reaction and SSA could take place at room temperature (27 °C), suggesting that the Cu(110)/Ta(111) interface is highly unstable. In addition, the chemical disordering artificially set in the Cu/Ta interface may also have some effects on the SSA of the Cu/Ta interface. First, for the Cu(111)/Ta(100) and Cu(111)/Ta(110) interfaces, even when the LRO parameter η is set to be 0 (corresponding to a completely disordered state), the interfacial reaction and SSA are reluctant to take place upon annealing up to a temperature of 600 °C. Second, for the Cu(100)/Ta(110), Cu(110)/Ta(110), and Cu(111)/Ta(111) interfaces, the interfacial reaction and SSA are also reluctant to take place upon annealing at 600 °C, when η is set to be 1 (corresponding to an entirely ordered crystalline state). Third, for the Cu(100)/Ta(100), Cu(100)/Ta(111), Cu(110)/Ta(100), and Cu(110)/Ta(111) interfaces, the interfacial reaction and SSA can take place even when η equals 1.

VI. CONCLUSION

(1) For the immiscible Cu-Ta system, the constructed Finnis-Sinclair is proven to be realistic, i.e., the Cu-Ta potential is not only able to reproduce some physical properties of some nonequilibrium Cu-Ta compounds, but also able to reflect some characteristic features of the Cu-Ta multilayers.

(2) Applying the Cu-Ta potential, MD simulation reveals that the interfacial texture plays an important role in influencing the solid-state reaction as well as the resultant SSA at the Cu/Ta interfaces. It is found that among the nine Cu/Ta interfaces stacked by possible combinations of (100), (110), and (111) atomic planes, the Ta (110) plane could all remain stable up to a temperature of 600 °C, while the Cu (111) plane remain unchanged only if combined with the Ta (100) and (110) planes.

(3) MD simulation also reveals that the interdiffusion of Cu and Ta atoms gives rise to the interfacial amorphization of the Cu/Ta interface, and that the diffusion of Ta into Cu is faster than the diffusion of Cu into Ta. The interface energy is therefore regarded as a major driving force for the interdiffusion and the resultant SSA.

(4) The amorphization energy of Cu is found to be less than that of Ta, resulting in an asymmetric growth behavior of SSA, i.e., in the Cu(100)/Ta(110) and Cu(110)/Ta(110) interfaces, SSA only takes place in the Cu lattice, and in the Cu(100)/Ta(100), Cu(100)/Ta(111), Cu(110)/Ta(100), Cu(110)/Ta(111), and Cu(111)/Ta(111) interfaces, SSA toward Cu is greater than that toward Ta.

ACKNOWLEDGMENTS

The authors are grateful to the financial support from the National Natural Science Foundation of China, The Ministry of Science and Technology of China (Grant No. G20000672), as well as from Tsinghua University.

*Author to whom correspondence should be addressed; Electronic mail: dmslbx@tsinghua.edu.cn

[1] R. B. Schwarz and W. L. Johnson, Phys. Rev. Lett. **51**, 415 (1983).
[2] B. X. Liu, W. S. Lai, and Z. J. Zhang, Adv. Phys. **50**, 367 (2001).
[3] F. R. deBoer, R. Boom, W. C. M. Mattens, A. R. Miedema, and A. K. Niessen, *Cohesion in Metals: Transition Metal Alloys* (North-Holland, Amsterdam, 1989).
[4] Q. Zhang, W. S. Lai, and B. X. Liu, Phys. Rev. B **58**, 14 020 (1998).
[5] Y. G. Chen and B. X. Liu, Appl. Phys. Lett. **68**, 3096 (1996).
[6] C. Lin, G. W. Yang, and B. X. Liu, Phys. Rev. B **61**, 15 649 (2000).
[7] K. Holloway and P. M. Fryer, Appl. Phys. Lett. **57**, 1736 (1990).
[8] C. Y. Chen, L. Chang, E. Y. Chang, S. H. Chen, and D. F. Chang, Appl. Phys. Lett. **77**, 3367 (2000).
[9] B. X. Liu, Z. J. Zhang, O. Jin, and F. Pan, in *Ion-Solid Interactions for Materials Modification and Processing*, edited by David B. Poker *et al.*, Mater. Res. Soc. Symp. Proc. No. 390 (Materials Research Society, Warrendale, PA, 1996), p. 71.
[10] K. W. Kwon, H. J. Lee, and R. Sinclair, Appl. Phys. Lett. **75**, 935 (1999).
[11] S. Li, Z. L. Dong, K. M. Latt, H. S. Park, and T. White, Appl. Phys. Lett. **80**, 2296 (2002).
[12] H. Ono, T. Nakano, and T. Ohta, Appl. Phys. Lett. **64**, 1511 (1994).
[13] K. M. Latt, Y. K. Lee, T. Osipowicz, and H. S. Park, Mater. Sci. Eng., B **94**, 111 (2002).
[14] H. R. Gong, and B. X. Liu, Appl. Phys. Lett. **83**, 4515 (2003).
[15] P. Heino, Comput. Mater. Sci. **20**, 157 (2001).
[16] H. R. Gong, L. T. Kong, W. S. Lai, and B. X. Liu, Phys. Rev. B **66**, 104204 (2002).
[17] M. W. Finnis and J. E. Sinclair, Philos. Mag. A **50**, 45 (1984).
[18] G. J. Ackland, G. Tichy, V. Vitek, and M. W. Finnis, Philos. Mag. A **56**, 735 (1987).
[19] Y. Kamimura, T. Tsutsumi, and E. Kuramoto, Phys. Rev. B **52**, 879 (1995).
[20] G. J. Ackland, D. J. Bacon, A. F. Calder, and T. Harry, Philos. Mag. A **75**, 713 (1997).
[21] G. Dagostino, Philos. Mag. B **76**, 433 (1997).
[22] T. Makino, K. Okouchi, and S. Matsuda, Mater. Trans., JIM **40**, 435 (1999).
[23] U. Kohler, C. Jensen, A. C. Schindler, L. Brendel, and D. E. Wolf, Philos. Mag. B **80**, 283 (2000).
[24] D. E. Luzzi, M. Yan, M. Šob, and V. Vitek, Phys. Rev. Lett. **67**, 1894 (1991).
[25] F. Ercolessi and J. B. Adams, Europhys. Lett. **26**, 583 (1994).
[26] G. Kresse and J. Hafner, Phys. Rev. B **47**, 558 (1993).
[27] J. Cai and Y. Y. Ye, Phys. Rev. B **54**, 8398 (1997).
[28] R. A. Johnson and D. J. Oh, J. Mater. Res. **4**, 1195 (1989).
[29] B. J. Lee, M. I. Bakes, H. Kim, and Y. K. Cho, Phys. Rev. B **64**, 184102 (2001).
[30] H. R. Gong, L. T. Kong, and B. X. Liu, Phys. Rev. B **69**, 054203 (2004).
[31] P. Mura, P. Demontis, G. B. Suffritti, V. Rosato, and M. Vittori Antisari, Phys. Rev. B **50**, 2850 (1994).
[32] B. M. Clemens, Phys. Rev. B **33**, 7615 (1986).
[33] C. Massobrio, V. Pontikis, and G. Martin, Phys. Rev. B **41**, 10 486 (1990).
[34] M. Parrinello and A. Rahman, J. Appl. Phys. **52**, 7182 (1981).
[35] S. R. Phillpot, S. Yip, and D. Wolf, Comput. Phys. **3**, 20 (1989).
[36] Y. Waseda, *The Structure of Non-Crystalline Materials: Liquid and Amorphous Solids* (McGraw-Hill, New York, 1980).
[37] V. Rosato, G. Ciccotti, and V. Pontikis, Phys. Rev. B **33**, 1860 (1986).
[38] W. K. Kuhn, R. A. Campbell, and D. W. Goodman, J. Phys. Chem. **97**, 446 (1993).
[39] R. Hoogeveen, M. Moske, H. Geisler, and K. Samwer, Thin Solid Films **275**, 203 (1996).
[40] Y. L. Chin, B. S. Chiou, and W. F. Wu, J. Appl. Phys. **41**, 3057 (2002).
[41] Z. J. Zhang, O. Jin, and B. X. Liu, Phys. Rev. B **51**, 8076 (1995).
[42] O. Jin, Z. J. Zhang, and B. X. Liu, Appl. Phys. Lett. **67**, 1524 (1995).
[43] H. J. Lee, K. W. Kwon, C. Ryu, and R. Sinclair, Acta Mater. **47**, 3965 (1999).